Supplementary information

High-resolution visualization of biofilm matrix development in space and time using fluorescent stains for cellulose

Zaira Heredia-Ponce[1], Aurélien Bailly [1,*] and Leo Eberl [1,*]

[1] Department of Plant and Microbial Biology, University of Zurich, Switzerland

*Corresponding authors: Department of Plant and Microbial Biology, University of Zürich, Zollikerstrasse 107, CH-8008 Zürich; Tel: +41 (0)44 63 48220; E-mail: aurelien.bailly@botinst.uzh.ch; leberl@botinst.uzh.ch

Supplementary Figures

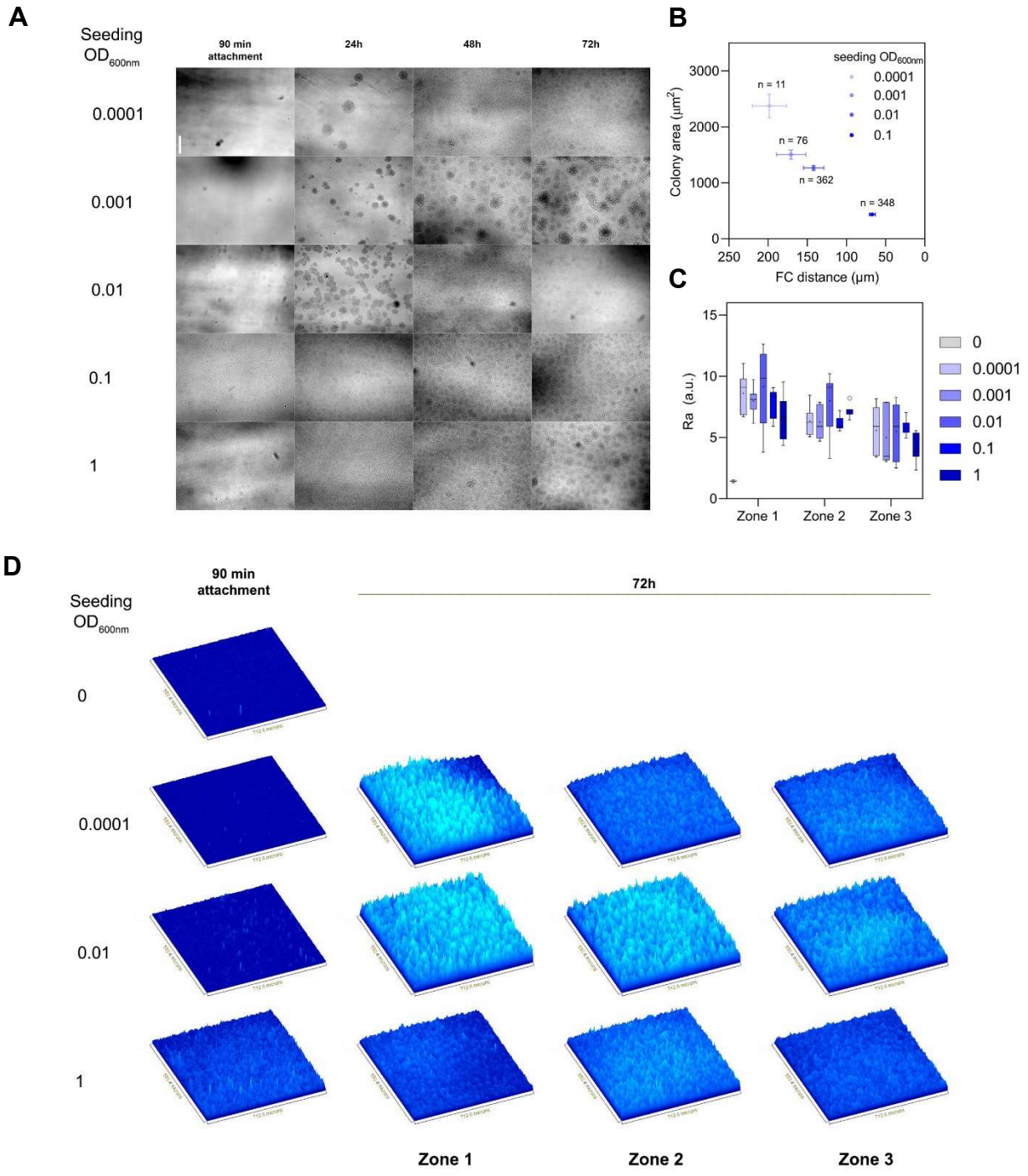

Supplementary Figure 1 | Seeding density determines flow-cell biofilm development. **A.** Representative bright field micrographs showing biofilms grown in Zone 1 (Fig. 1A) at the given time points. Bar = 100 µm. **B.** Colony area in 24h biofilms in function to FC distances after 90 min attachment, sample sizes, means and s.e.m. are given. **C.** Arithmetic roughness means of 72h biofilms surfaces at the specified seeding density measured with the FiJi SurfCharJ 1q plugin (n = 6-9). Zones 1-3 correspond to those described in Fig. 1A. **D.** Surface plots of representative biofilms at the given time points, sampling zones and seedings densities.

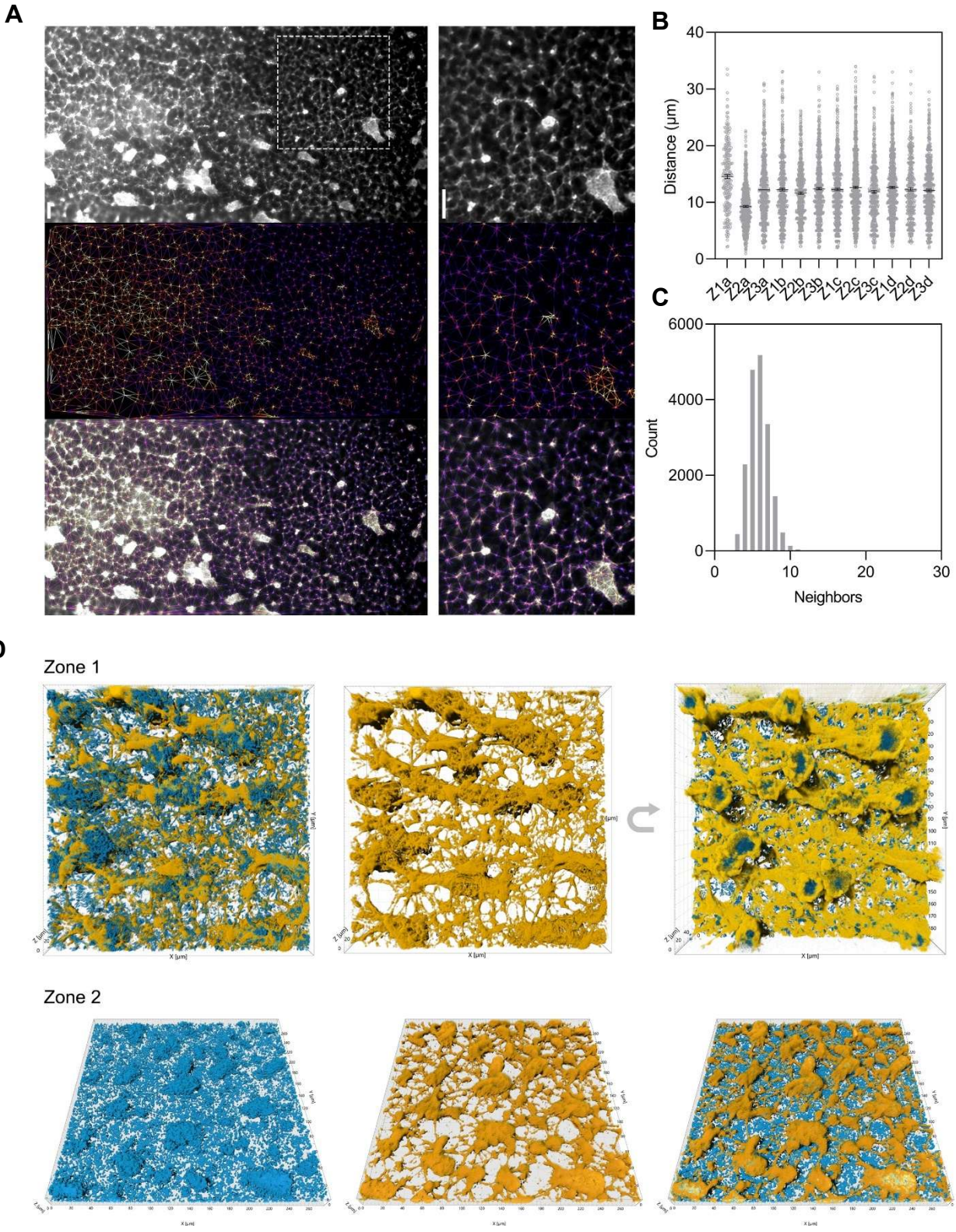

Supplementary Figure 2 | The isoF ECM is an extended, continuous network covering the whole substratum. A. Delaunay triangulation analysis from ECM nodes (maxima). Top, acquired epifluorescence micrograph. Middle, resulting difference image between the micrograph and Delaunay diagram, Fire LUT. Bottom, overlay of both images. Bar = 25 µm. **B.** Mean neighbour-neighbour distances. Four independent replicates (a-d) were sampled in the zones described in Fig. 1A (Z1 = zone 1, Z2 = zone 2 and Z3 = zone 3). **C.** Distribution of nearest-neighbours number from pooled samples a-d. Typically, one node connects 4-8

neighbours. **D.** Shadow projections of representative Zone 1 and Zone 2 biofilms (Fig. 1A). IsoF cells are shown in blue and the ECM in yellow. Zone 1 sample is viewed through the glass substratum and flipped around the Y axis as indicated. Zone 2 sample is viewed from the inner chamber to the glass substratum. Note the regular ECM connectivity between small and large microcolonies.

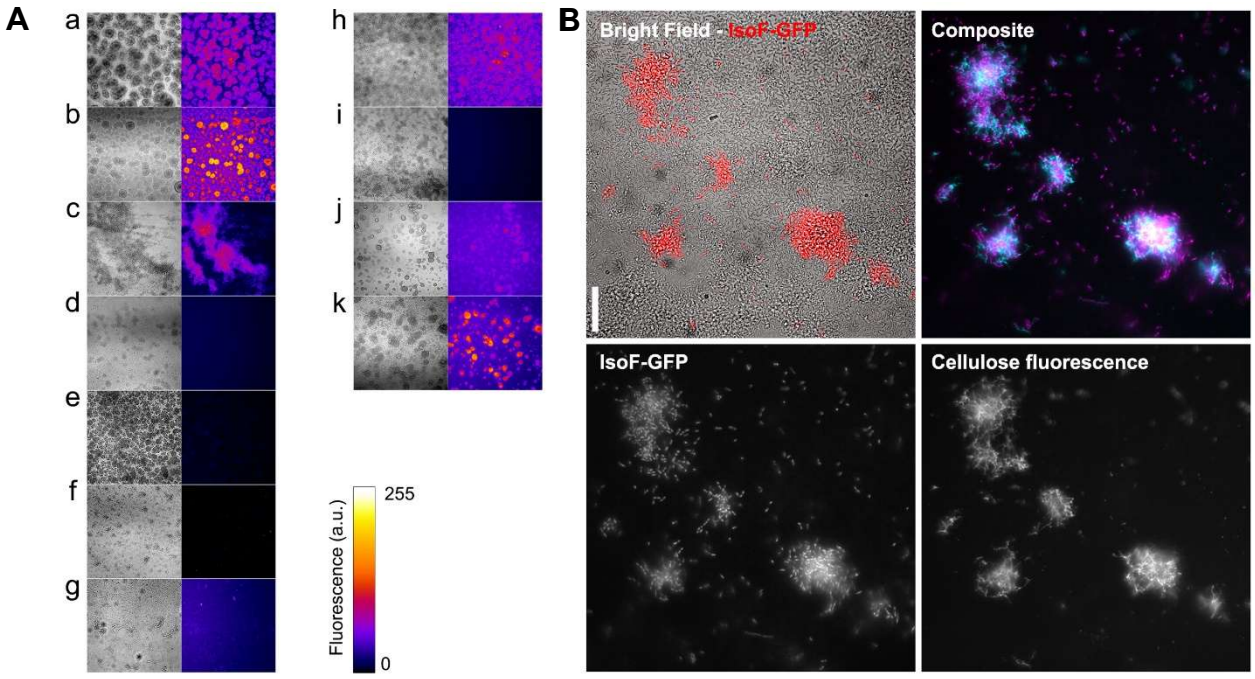

Supplementary Figure 3 | Compound (1) demonstrates specificity towards the extracellular matrices of bacterial strains potentially producing cellulose as their prominent exopolysaccharide.

A. Mature flow-cell wildtype biofilms grown in the constant presence of compound (**1**). **a,** *Pseudomonas sp. IsoF* (cellulose)*;* **b,** *Pseudomonas syringae pv. syringae* UMAF0158 (cellulose); **c,** *Pseudomonas syringae pv. tomato* DC3000 (cellulose); **d,** *Pseudomonas aeruginosa* PAO1 (Psl); **e,** *Pseudomonas simiae* WCS417r (EPS I). **f,** *Pseudomonas chlororaphis* PCL1606 (Psl); **g,** *Pseudomonas protegens* CHA0 (Pel or Psl); **h,** *Burkholderia vietnamiensis* LMG18836 (cellulose); **i,** *Ralstonia solanacearum* (EPS); **j,** *Pandoraea sputorum* (cellulose); **k,** *Enterobacter sakazakii* ATCC29004 (cellulose). The putative exopolysaccharide name for each strain is given into brackets. Left, bright field, gray levels; right, compound (**1**) fluorescence, Fire LUT. Bar = 20 µm. **B.** Representative micrographs of a mature flow-cell IsoF-GFP / *P. chlororaphis* PCL1606 mixed biofilm (2-days old). To distinguish the non-fluorescent wildtype PCL1606 strain from GFP-expressing IsoF, the GFP fluorescent signal (red) was overlaid to the bright field image (gray). Note that the compound (**1**) fluorescent signal revealing cellulose fibres localizes with IsoF-GFP aggregates. Bar = 25 µm.

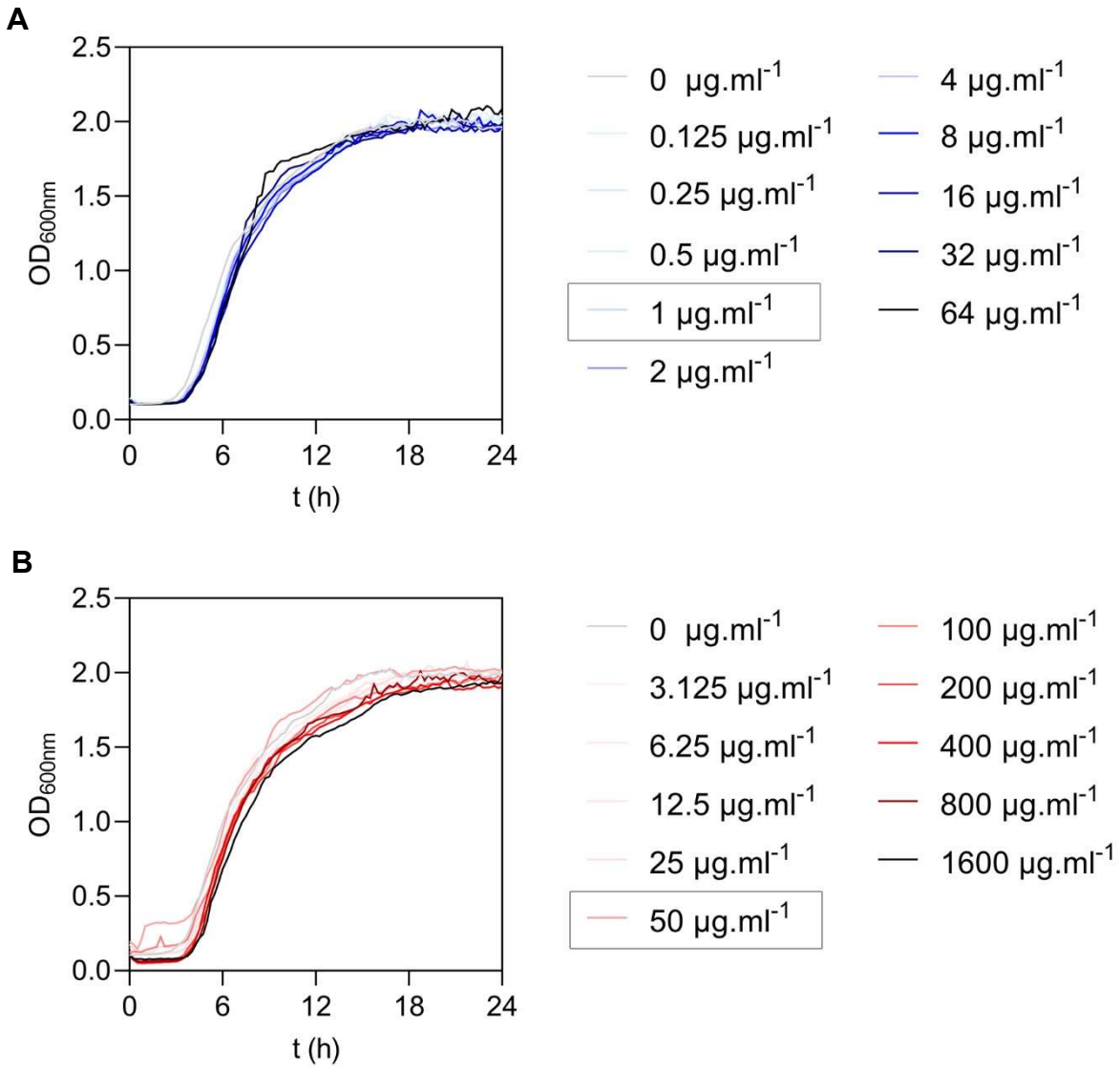

Supplementary Figure 4 | Growth of IsoF wt strain in the presence of increasing concentrations of the compound (1) and compound (2) fluorescent probes. A. Growth of wildtype IsoF in the presence of compound (**1**) fluorescent probe (n = 3). **B.** Growth of wildtype IsoF in the presence of compound (**2**) fluorescent probe (n = 3). None of the concentrations impairs cell growth. Gray boxes indicate working concentrations allowing visualization of polysaccharidic fibres with good photostability and signal-to-background ratio.

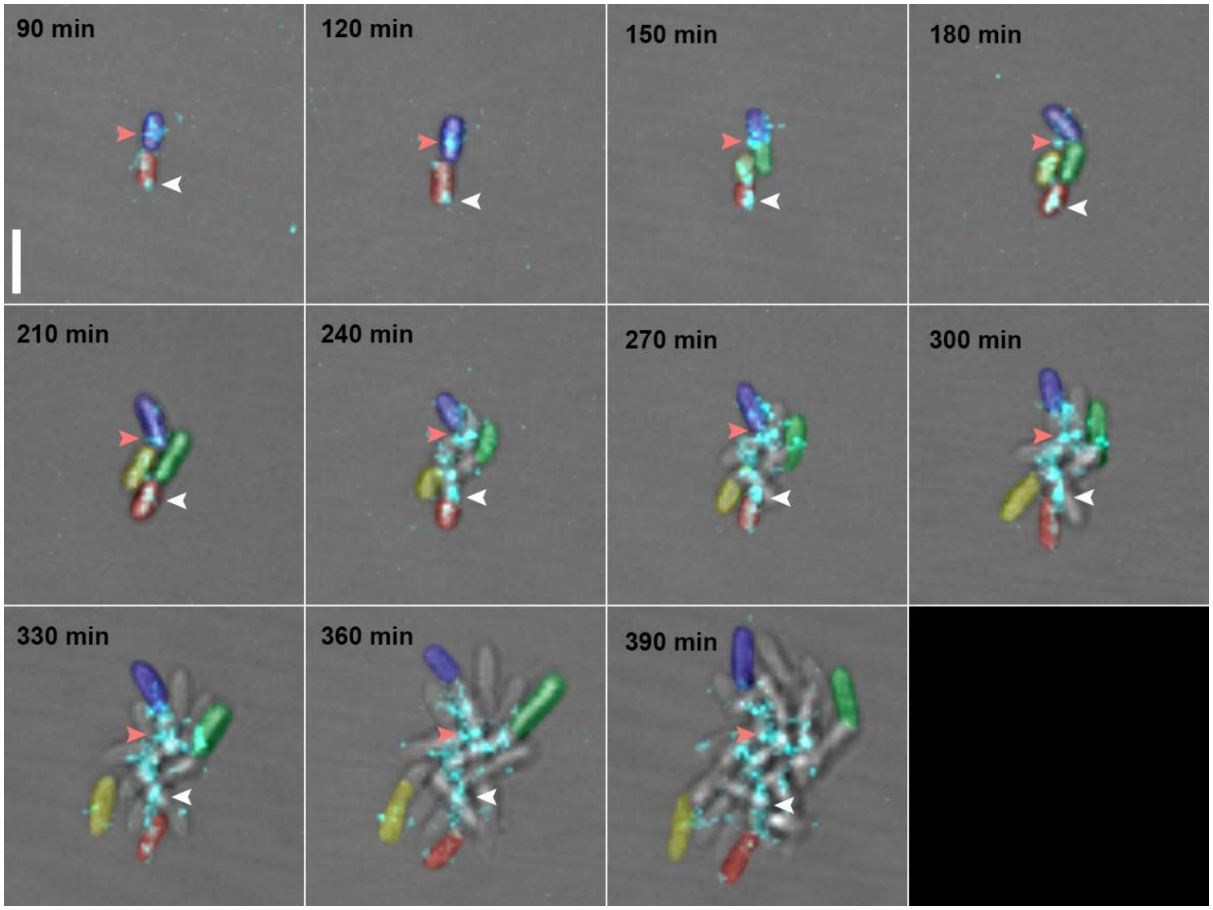

Supplementary Figure 5 | FC populations rapidly secure anchorage to the glass substratum by cellulose deposition. Montage of the first 5 h of aggregate formation following a 90 min attachment period. CLSM acquisitions displaying BF transmission image and cellulose fluorescence signal overlay (cyan). The arrowheads indicate initial cellulose depositions along the sequence. The first two external progenies have been coloured for visibility. Bar = 5 µm

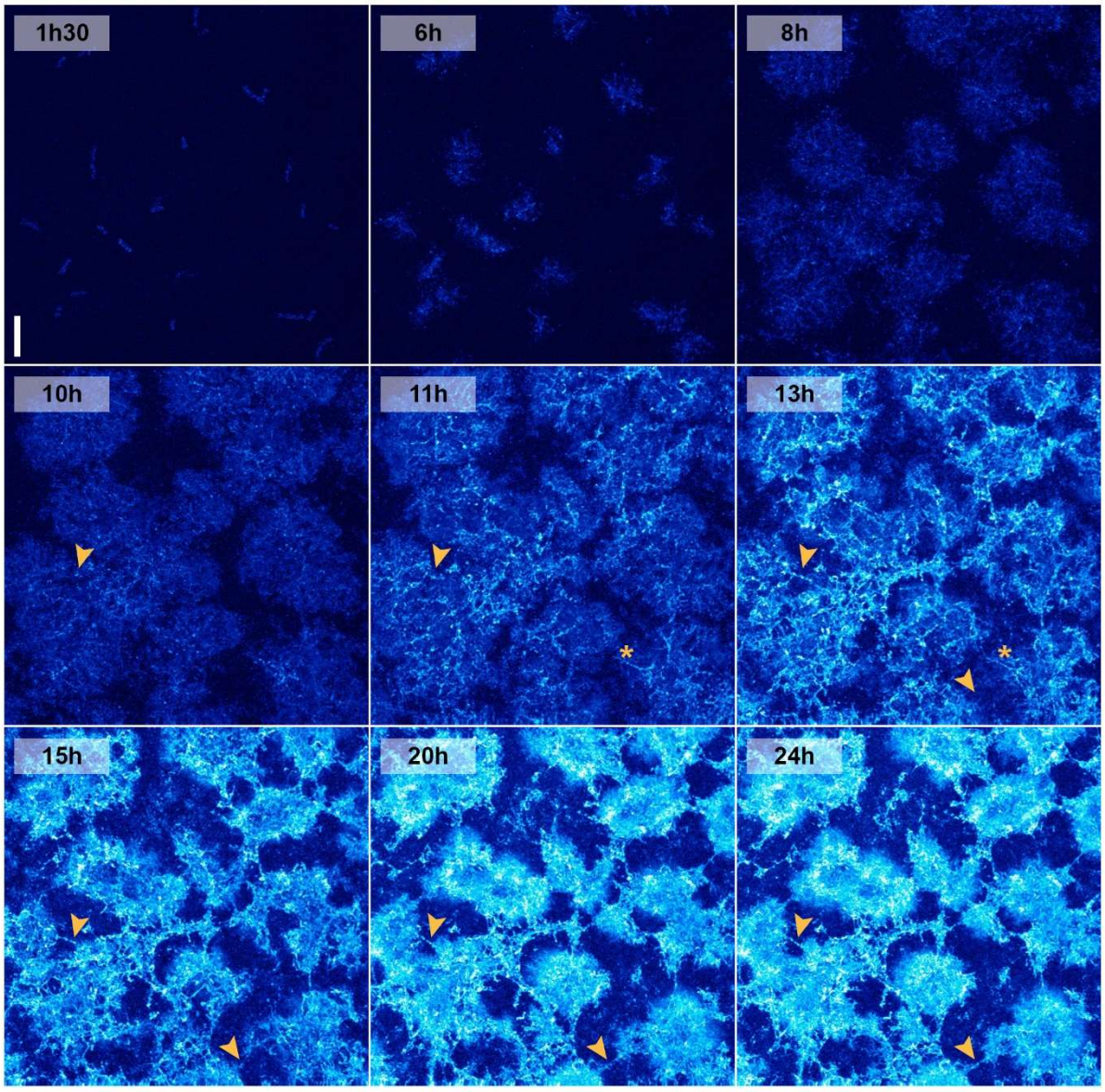

Supplementary Figure 6 | The cellulose network self-reorganizes into a fibrous lattice within few hours. CLSM maximum projections of IsoF temporal matrix development following FC attachment. Cellulose fluorescence in the presence of compound **(1)** is displayed in blue. Arrowheads indicate locations of fibres establishment. Asterisks point to an unstable fibre. Bar = 10 µm.

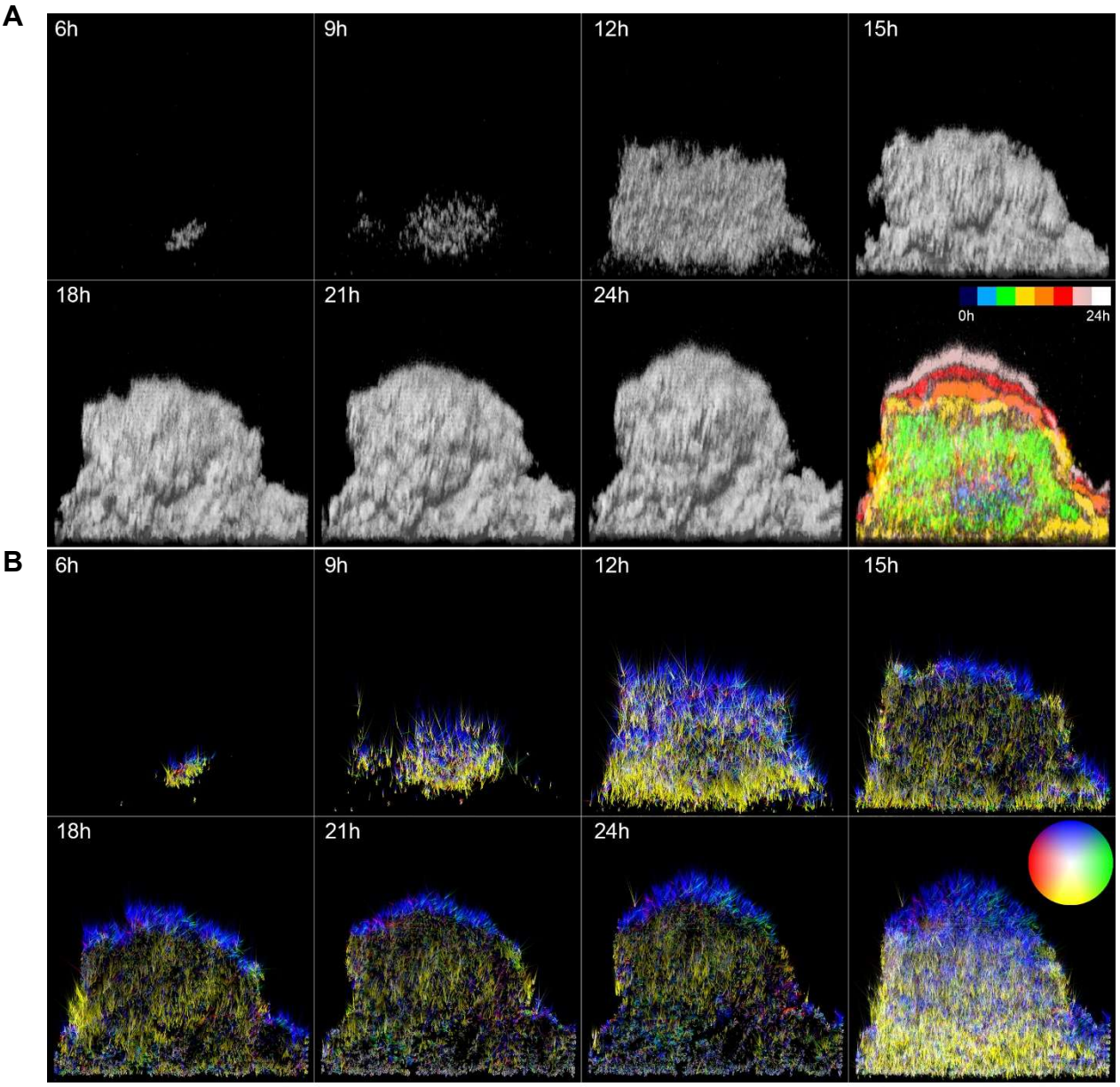

Supplementary Figure 7 | Anisotropic cellulose production and self-organized remodelling frame the emergence of the canonical mushroom-like structure. A. Temporal dynamics of cellulose production in IsoF flow-cell biofilm at the given time points.

The false-coloured temporal projection displays the progression of cellulose production in 4 h intervals. **B.** Lukas-Kanade optical flow maps at the given time points; DC 2D noise mapping. The last frame displays the maximum projection of each map and the colour wheel indicates directions and magnitudes. Growth of the microcolony was recorded for 24 h at 30 min intervals. See Suppl. Video 6. Bar = 20 um. **C.** A diagram depicting the apparent EPS dynamics giving rise to mushroom-like shaped colonies. Cellulose was stained with compound (**2**).

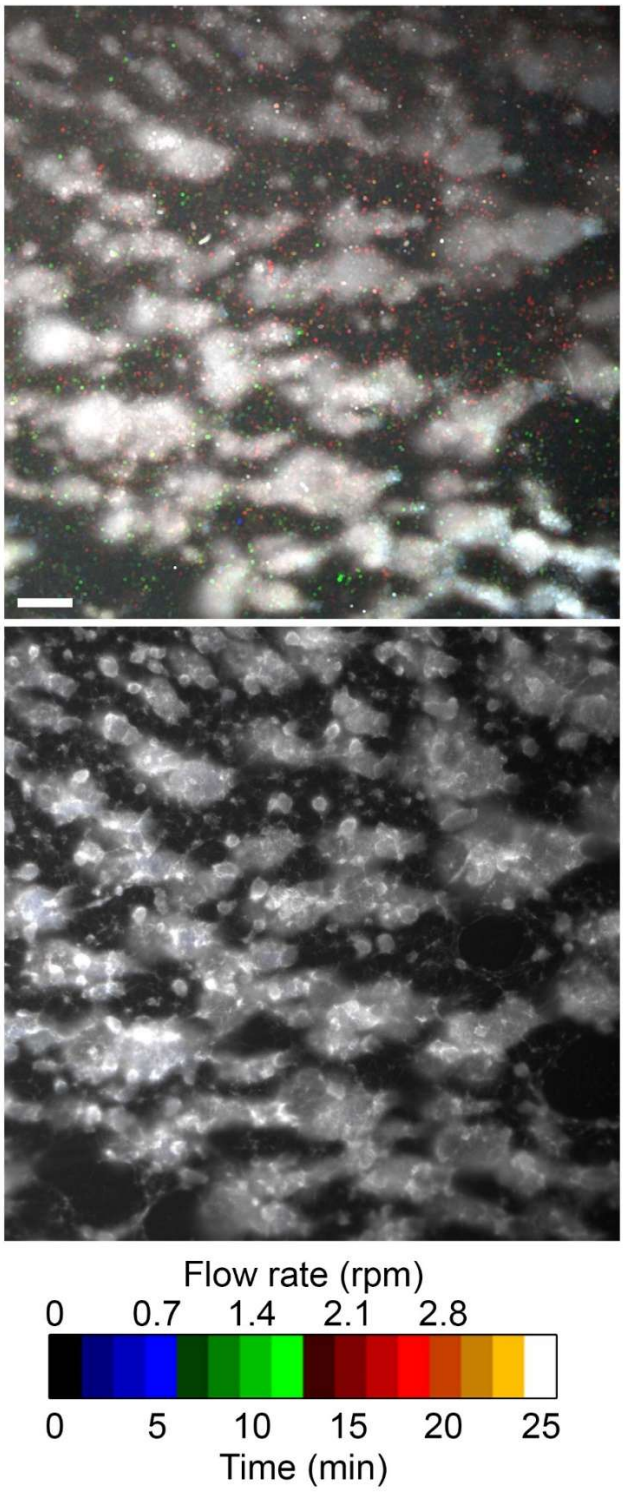

Supplementary Figure 8 | The cellulose matrix displays remarkable stability under increasing flow rates. Temporal maximum projection of a 25 min acquisition (10 seconds/frame) under the epifluorescence microscope. The flow rate of the pump doubles every 5 minutes. Top, IsoF wildtype cells, Syto9 fluorescence; Bottom, cellulose fluorescence. Cell signals were enhanced (Maximum filter, 2 pixels radius) for better visualization. Free cells washed away along the flow appear in green, red or yellow shades, while ECM-embedded cells appear white, indicating stationary positions. Note the structural resilience of the cellulose network. Bar = 50 µm.

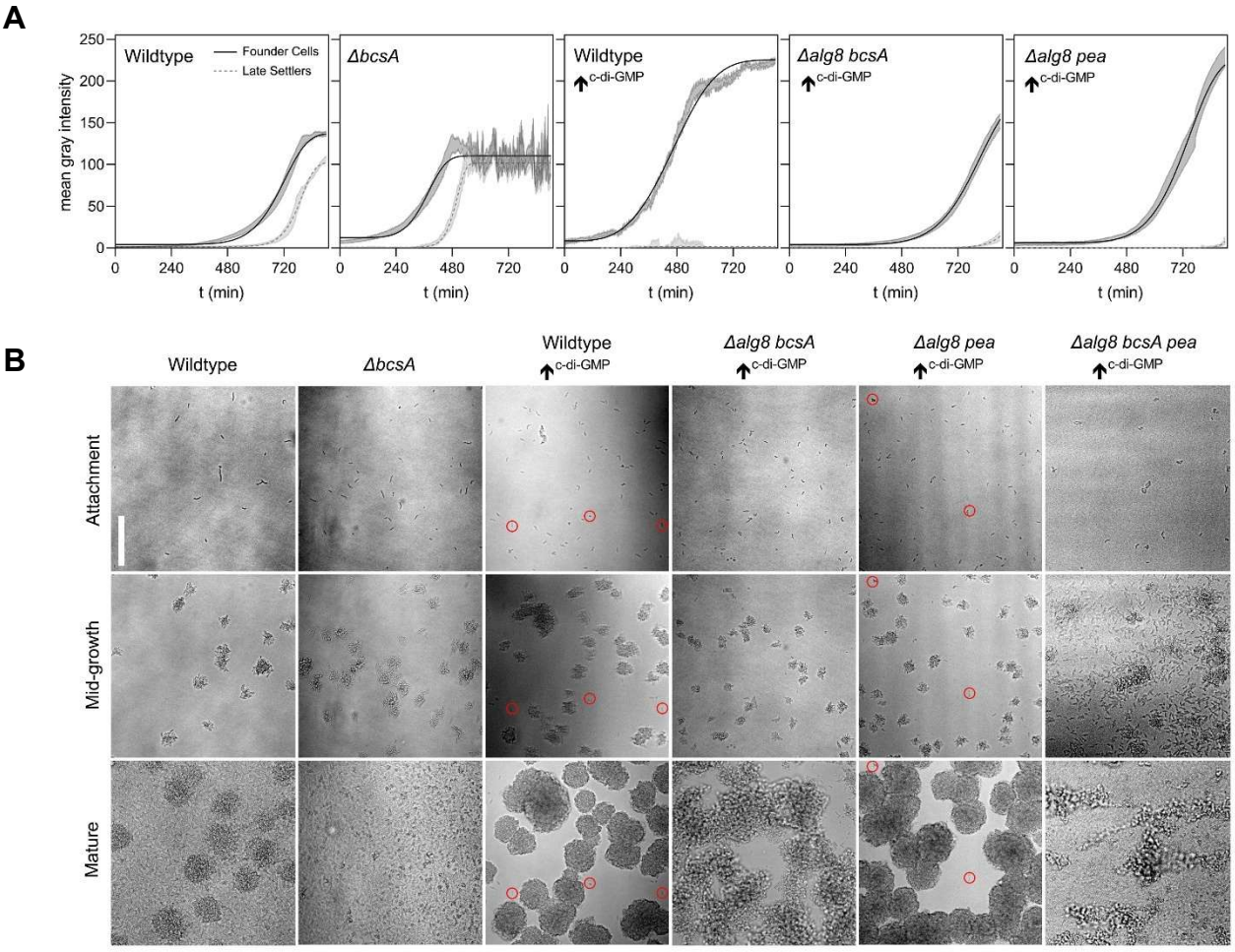

Supplementary Figure 9 | Elevated c-di-GMP levels lead to dense microcolony formation in flow-cell biofilms. A. Temporal FC and LS microcolonies cell density estimated from Bright Field acquisitions. Note that both cellulose (*Δalg8,pea* ↑c-di-GMP) and Pea (*Δalg8,bcsA* ↑c-di-GMP) overproduction prevent the appearance of LS populations. Weibull growth non-linear fit, n = 8, s.e.m. is given as gray shade. **B.** Micrographs of representative biofilms of the given strains at discrete time points. Red circles indicate the positions of FCs that did not develop into large aggregates and thus are not LS cells. Note that cellulose and/or Pea overproduction through high c-di-GMP levels do not contain LS cells between microcolonies. Bar = 50 µm

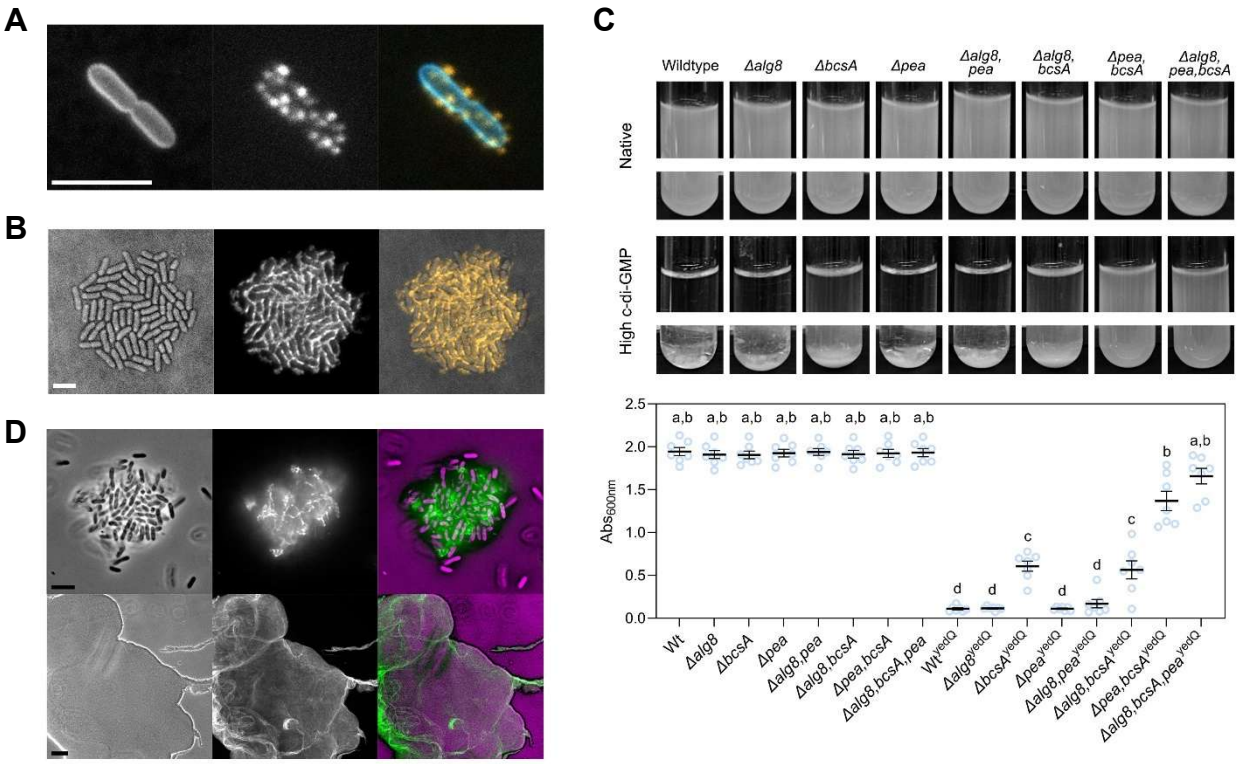

Supplementary Figure 10 | Cellulose and/or Pea overproduction lead to an autoaggregative phenotype in IsoF. A. Wt^{yedQ} single cells (left, FM4-64 membrane staining) display globular patterns of cellulose production sites (middle, compound **(1)** fluorescence) scattered on their surfaces (right, overlay). Bar = 5 µm, **B.** Single Wt^{yedQ} cells grow in 2D radial patterns (left, transmission channel) on nutrient agar patches and encase themselves into a dense cellulose matrix (middle, compound **(2)** fluorescence) that ensures a tight connection between daughter cells (right, overlay). Bar = 5 µm. **C.** Representative images of overnight cell cultures grown at 30°C and 220 rpm of IsoF wildtype and its derived polysaccharide mutant strains under native and high c-di-GMP levels. The graph displays the mean absorbance at 600 nm wavelength of cultures sampled from the liquid column. Different letters indicate statistically significant differences ($p \leq 0.05$, one-way ANOVA with Tukey's post-hoc test, n = 6). **D.** Wt^{yedQ} cultures contain small (top) and large (bottom) cellular aggregates encased in a dense cellulose matrix. From left to right: Bright field Wt^{yedQ} cells, compound **(1)** fluorescence, overlay. Bars = 5 and 20 µm, respectively.

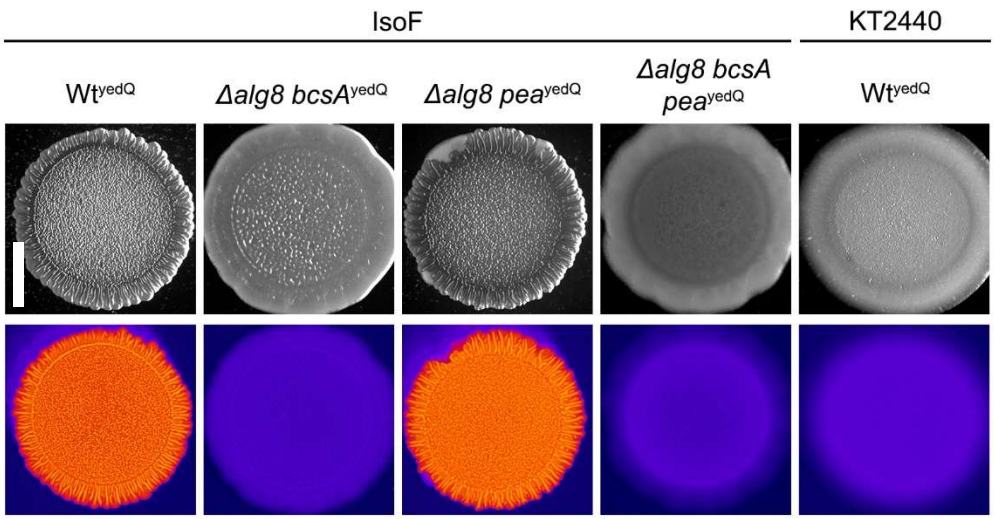

Supplementary Figure 11 | The model strain *P. putida* KT2440 seems impaired in cellulose production. Macrocolonies of the specified wildtypes and polysaccharide mutant strains under high c-di-GMP conditions were grown for 5 days on solid LB medium supplemented with compound (**2**). Top, Bright Field image; bottom, compound (**2**) specific cellulose fluorescence, Fire LUT. Note the absence of the typical rugose morphology and stained cellulose fluorescence in KT2440 under high c-di-GMP conditions. Bar = 5 mm.

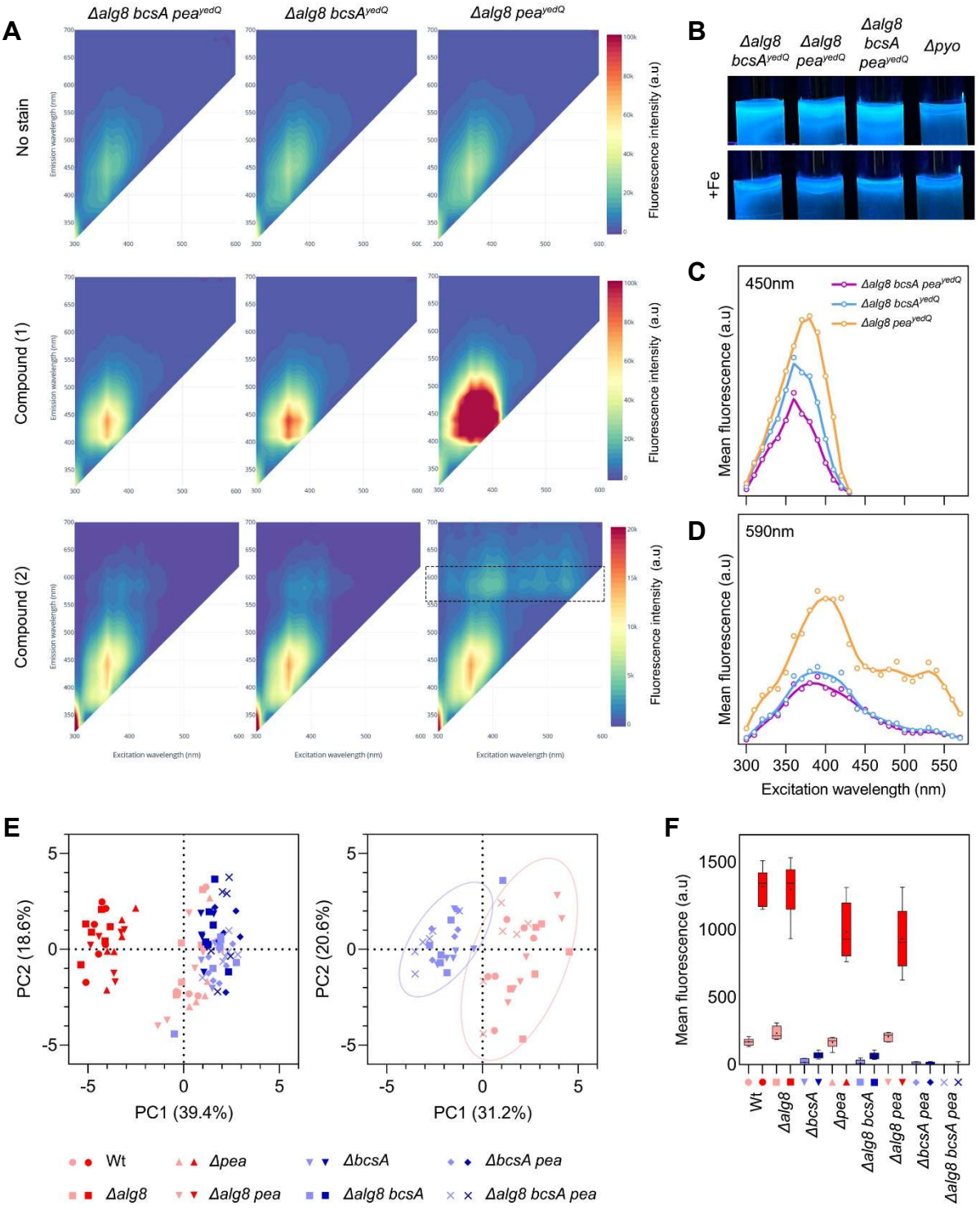

Supplementary Figure 12 | Compounds (1) and (2) demonstrate specificity towards cellulose in IsoF pellicles. A. λ^2 contour maps of the spectral properties of given mutant IsoF pellicles. The dashed box indicates compound (**2**) specific cellulose fluorescence **B.** Native fluorescence of given mutant IsoF pellicles when excited at 366 nm; note the decrease in fluorescence to the pyoverdine-free mutant level (*Δpyo*) in iron-replete conditions. **C.** Compound (**1**) mean fluorescence intensities of labelled pellicles at 450 nm emission; note that the cellulose-specific signal overlaps background fluorescence. **D.** Compound (**2**) mean fluorescence intensities of labelled pellicles at 590 nm emission; the cellulose-specific signal

readily separates from background fluorescence. **E.** Principal Component Analyses of microscopic acquisitions features of the given wildtype and mutant IsoF pellicles (n = 6). Red hues indicate the presence of cellulose, blue hues indicate its absence. Darker hues denote high c-di-GMP conditions. The left graph includes all samples; the right graph represents the analysis of strains under native c-di-GMP conditions only. The 95% confidence intervals are marked by oval circles. **F.** Specific compound (**2**) mean fluorescence of the given strains.

Supplementary Tables

Supplementary Table 1. Bacterial strains used in this study.

Strain	Annotation	Description	Reference
Pseudomonas sp. IsoF	Wt	Wildtype strain	Steidle *et al.,* 2001
Pseudomonas sp. IsoF *Δalg8*	*Δalg8*	Deletion mutant (*PisoF_02555 gene*) impaired in alginate production	This study
Pseudomonas sp. IsoF *ΔbcsA*	*ΔbcsA*	Deletion mutant (PisoF_03918 gene) impaired in cellulose production	This study
Pseudomonas sp. IsoF *Δpea*	*Δpea*	Deletion mutant (PisoF_04500-PisoF_04518) impaired in Pea polysaccharide production	This study
Pseudomonas sp. IsoF *Δalg8,bcsA*	*Δalg8,bcsA*	Double deletion mutant impaired in alginate and cellulose production	This study
Pseudomonas sp. IsoF *Δalg8,pea*	*Δalg8,pea*	Double deletion mutant impaired in alginate and Pea production	This study
Pseudomonas sp. IsoF *ΔbcsA,pea*	*ΔbcsA,pea*	Double deletion mutant impaired in cellulose and Pea production	This study
Pseudomonas sp. IsoF *Δalg8,bcsA,pea*	*Δalg8,bcsA,pea*	Triple deletion mutant impaired in alginate, cellulose and Pea production	This study
Pseudomonas sp. IsoF *ΔPisoF_03915*	*Δ PisoF_03915*	Deletion mutant in the gene immediately upstream the cellulose cluster (gene *PisoF_03915*)	This study

Pseudomonas sp. IsoF pBBR1MCS5 *yedQ*	Wt^{yedQ}	IsoF wildtype strain overexpressing the diguanylate cyclase *yedQ* (expected high c-di-GMP levels)	This study
Pseudomonas sp. IsoF pBBR1MCS5 *PisoF_03915*	Wt^{PisoF_03915}	IsoF wildtype strain overexpressing the diguanylate cyclase *PisoF_03915* (expected high c-di-GMP levels)	This study
Pseudomonas sp. IsoF *Δalg8* pBBR1MCS5 *yedQ*	$\Delta alg8^{yedQ}$	Strain impaired in alginate production overexpressing *yedQ* (expected high c-di-GMP levels)	This study
Pseudomonas sp. IsoF *ΔbcsA* pBBR1MCS5 *yedQ*	$\Delta bcsA^{yedQ}$	Strain impaired in cellulose production overexpressing *yedQ* (expected high c-di-GMP levels)	This study
Pseudomonas sp. IsoF *Δpea* pBBR1MCS5 *yedQ*	Δpea^{yedQ}	Strain impaired in Pea polysaccharide production overexpressing *yedQ* (expected high c-di-GMP levels)	This study
Pseudomonas sp. IsoF *Δalg8,bcsA* pBBR1MCS5 *yedQ*	$\Delta alg8,bcsA^{yedQ}$	Double deletion mutant overexpressing *yedQ* (expected high c-di-GMP levels)	This study
Pseudomonas sp. IsoF *Δalg8,pea* pBBR1MCS5 *yedQ*	$\Delta alg8,pea^{yedQ}$	Double deletion mutant overexpressing *yedQ* (expected high c-di-GMP levels)	This study
Pseudomonas sp. IsoF *ΔbcsA,pea* pBBR1MCS5 *yedQ*	$\Delta bcsA,pea^{yedQ}$	Double deletion mutant overexpressing *yedQ* (expected high c-di-GMP levels)	This study
Pseudomonas sp. IsoF *Δalg8,bcsA,pea* + pBBR1MCS5 *yedQ*	$\Delta alg8,bcsA,pea^{yedQ}$	Triple deletion mutant overexpressing *yedQ* (expected high c-di-GMP levels)	This study

Supplementary Table 2. Plasmids used in this study. Trimethoprim (Tp), tetracycline (Tc), gentamycin (Gm), kanamycin (Km). ^{R} stands for resistance.

Plasmid	Description	Reference
pGPI-SceI::Tet	Suicide plasmid with oriR6K, mob^{+}, I-SceI restriction site; Tp^{R} Tc^{R}	Purtschert *et al.,* 2022
pGPI::Tet-*alg8*	pGPI-SceI-Tet plasmid with fused regions flanking the *alg8* gene	This study
pGPI::Tet-*bcsA*	pGPI-SceI-Tet plasmid with fused regions flanking the *bcsA* gene	This study
pGPI::Tet-*pea*	pGPI-SceI-Tet plasmid with fused regions flanking the *pea* cluster	This study
pGPI::Tet-*PisoF_03915*	pGPI-SceI-Tet plasmid with fused regions flanking the *PisoF_03915* gene	This study
pDAI-SceI::Gm	pDA17 plasmid carrying the I-SceI nuclease gene; Gm^{R}	Flannagan *et al.,* 2008
pRK2013	Helper plasmid; RK2 derivative, mob^{+} tra^{+} ori ColE1; Km^{R}	Figurski *et al.,*1979
pBBR1MCS5 *yedQ*	pBBR1MCS5 plasmid with the *yhcK* gene of *E. coli* TG1 strain	Steiner *et al.,* 2022
pBBR1MCS5 *PisoF_03915*	pBBR1MCS5 plasmid with PisoF_03915 gene of IsoF	This study

Supplementary Table 3. Primers used in this study; ✦ size expected in wildtype genotype, ✧ size expected in mutant genotype, ✣ higher than 10 kb in the wildtype. Letters in italics represent restriction sites.

Primer	Sequence	Description	Size (bp)	Reference
*alg8*_up_fw_KpnI	AAAAAA*GGTACC*GCTGAACCTGTCCCAGTACT	To amplify the region upstream *alg8* gene	636	This study
*alg8*_up_rv_NcoI	AAAAAA*CCATGG*CGCGAAATCAGGGAAGGAAG			
*alg8*_dw_fw_NcoI	AAAAAA*CCATGG*GCTGTTCATGGTCGTGTGAG	To amplify the region downstream *alg8* gene	699	This study
*alg8*_dw_rv_EcoRI	AAAAAA*GAATTC*CTTTCGACCAGGCTGTTCAC			
*bscA*_up_fw_KpnI	AAAAAA*GGTACC*GTGCTGTTGATCGACCTGTG	To amplify the region upstream *bcsA* gene	635	This study
*bscA*_up_rv_NcoI	AAAAAA*CCATGG*GTAAGCCGACAGAGGGTTCA			
*bscA*_dw_fw_NcoI	AAAAAA*CCATGG*ATCGAGACGCATGATGACTG	To amplify the region downstream *bcsA* gene	570	This study
*bscA*_dw_rv_EcoRI	AAAAAA*GAATTC*AAGTACGCCAGGTCGTTGTC			
*pea*_up_fw_KpnI	AAAAAA*GGTACC*AGCCACGTACACCCAGAAAC	To amplify the region upstream *pea* gene cluster	549	This study
*pea*_up_rv_NcoI	AAAAAA*CCATGG*GTCCAGGCGGTATTGAGAAA			
*pea*_dw_fw_NcoI	AAAAAA*CCATGG*GCCTTTATTCGCAAGACCAG	To amplify the region downstream *pea* gene cluster	533	This study
*pea*_dw_rv_EcoRI	AAAAAA*GAATTC*CTGCTCAACGATGAACTGGA			
*PisoF_03915*_up_fw_KpnI	AAAAAA*GGTACC*CGCGTTGCAGATGGAGATTG	To amplify the region upstream the *PisoF_03915* gene	503	This study
*PisoF_03915*_up_rv_NcoI	AAAAAA*CCATGG*TGACGCTATCTATCGGTGTGG			
*PisoF_03915*_dw_fw_NcoI	AAAAAA*CCATGG*TCAAAATCAGGCCACGCAGG	To amplify the region downstream the *PisoF_03915* gene	610	This study
*PisoF_03915*_dw_rv_EcoRI	AAAAAA*GAATTC*GCGTGAGGGTTGGCTTCATA			

*alg8*_out_fw	ACCTGGGCCTTGAGTACATC	To check *alg8* deletion	3787 ✦	This study
*alg8*_out_rv	GCTTTGTCGATCAGCCAGTT		2317 ✧	
*bcsA*_out_fw	ACCAGTTACCTGGCGTTGTC	To check *bcsA* deletion	4998 ✦	This study
*bcsA*_out_rv	GCATGCTGGTGATGTACTGG		2435 ✧	
*pea*_out_fw	AGCATGGCATCCTTGAAGTC	To check *pea* cluster deletion	✣	This study
*pea*_out_rv	CCTGCGTTCTATTCCGTCAT		1955 ✧	
*PisoF_03915*_out_fw	TCGGTGACATGCTCGTAGG	To check *PisoF_03915* deletion	3253 ✦	This study
*PisoF_03915*_out_rv	CTTTGCCGCGATACACCTG		1879 ✧	
*PisoF_03915*_fw_HindIII	AAAA*AAGCTT*ATGGGCAACATTCTGTCATC	To overexpress *PisoF_03915* in the pBBR1MCS5 plasmid	1572	This study
*PisoF_03915*_rv_BamHI	AAAA*GGATCC*CTAGGAAGGCACGCGATCTT			

Supplementary videos

Supplementary Video S1 | Image sequence used to build figure 1B. Two IsoF cells initially attached to the glass surface (FC) generate a microcolony. The first daughter LS cell exits the FC microcolony at 1:05.14. Field of view is 96 x 39 µm. 60 fps, 5s per frame.

Supplementary Video S2 | A prolonged laser excitation generates stress on the microcolony and destabilizes its ECM (green). The arrow indicates a magenta-highlighted single cell that actively swims away from the FC microcolony ECM at 3.5 min. Field of view is 90 x 90 µm. 5 fps, 5s per frame.

Supplementary Video S3 | Cellulase treatment disrupts the IsoF extracellular matrix. Cultures were incubated overnight (16h) in presence (top) or absence (bottom) of cellulase. Flow and recording were started at the same time with the same rate. Note the high biofilm stability conferred by the cellulose network.

Supplementary Video S4 | **2D dynamics of wildtype IsoF flow-cell biofilm development in 72 h.** Temporal epifluorescence microscopic acquisition. Surface-liquid interface view; the focus plane was set on the FC population prior to acquisition. Note the synchronicity of cellulose production among FC aggregates and the gradual colonization of the substratum by LS cells. After 24 h of growth, the biofilm appears mature and stable. Top, grayscale Bright Field, IsoF wildtype cells; Red overlay, cellulose fluorescence. Bottom, grayscale cellulose fluorescence. The changes in cellulose signal intensities at 24 h and 48 h are due to adjustments in fluorescence acquisition settings. Field of view = 712x532 µm. 10 min per frame .

Supplementary Video S5 | **Cellulose fibrils self-organize into tensed structures.** Temporal CLSM acquisition of cellulose fluorescence; left, original acquisition; right, contrast enhanced data. The sequence shows how cellulose-cellulose interactions model the condensed final lattice. Field of view = 80x80 µm.

Supplementary Video S6 | **Anisotropic cellulose production and convective-like remodelling frame the emergence of the canonical mushroom-like structure.** Growth of a microcolony recorded for 24 h at 30 min intervals, as observed in Suppl. Video 6; cellulose fluorescence, resliced CLSM acquisitions. This material was used to prepare Suppl. Fig. 7.

Supplementary Video S7 | **2D dynamics of IsoF ∆*bcsA* mutant flow-cell biofilm development in 72 h.** Temporal epifluorescence microscopic acquisition. Surface-liquid interface view; the focus plane was set on the FC population prior to acquisition. Note the absence of cellulose production compared to Suppl. Video 7. The absence of cellulose leads to biofilm collapse driven by flow shear forces. ∆*bcsA* cells retain their capacity to adhere to the substratum. Grayscale Bright Field, IsoF ∆*bcsA* cells; Red overlay, cellulose fluorescence. Field of view = 712x532 µm. 10 min per frame .

Supplementary Video S8 | **Dynamics of 48h pellicle formation at the surface of a multiwell plate.** IsoF wildtype cells expressing *GFP* are shown in magenta, cellulose fluorescence in green. Note the synchronous emergence of the cellulose network linking small aggregates and bigger microcolonies at the air-liquid interface. The movements of motile cells beneath the pellicle can easily be observed. Field of view is 6.8 x 5.1 mm.

Supplementary Video S9 | **Cellulose or Pea-based pellicles formed by IsoF under high c-di-GMP levels.** Note that the cellulose-based pellicle is considerably more fragile and visually exhibits a weaker consistency compared to the Pea-based pellicle.

Supplementary Video S10 | Pellicle spatiotemporal development in glass tubes. Standing cultures of the given strains were grown for 48h. Note the near synchronous collapse of pellicles that do not produce Pea.